

Mechanical Properties of Four 7-9%Cr Reduced Activation Martensitic Steels after 2.5 dpa, 300°C Irradiation⁴

Reference: van Osch, E., Horsten, M., Lucas, G. E., and Odette, G. R., “Mechanical Properties of Four 7-9%Cr Reduced Activation Martensitic Steels after 2.5 dpa, 300°C Irradiation,” *Effects of Radiation on Materials: 19th International Symposium, ASTM STP 1366*, M. L. Hamilton, A. S. Kumar, S. T. Rosinski, and M. L. Grossbeck, Eds., American Society for Testing and Materials, West Conshohocken, PA, 2000.

Abstract: Reduced Activation Ferritic/Martensitic alloys are being developed for application in future thermonuclear fusion reactors. The behavior of the reduced activation martensitic steel F82H-mod was compared with small amounts of related alloys JLF-1, JLF-1B and ORNL-9Cr2WVTa, following irradiation in the High Flux Reactor (HFR) in Petten. Tensile, KLST-type Charpy impact and CT fracture toughness mechanical properties specimens, were neutron irradiated to a dose level of 2-3 dpa at 300°C. Results of post irradiation tensile, miniaturized charpy impact, and static fracture toughness tests are presented and interpreted in terms of irradiation hardening and irradiation induced shift of ductile to brittle transition temperature (DBTT) and reduction of upper shelf energy (USE). The observed irradiation hardening (140 – 170 MPa at 300°C) is moderate, whereas the observed radiation induced shift in DBTT is approximately 150°C for KLST-type impact test specimens for F82H. Similar observations are made for the static fracture toughness tests. For JLF-1B the irradiation hardening is one third higher than for JLF-1, and shift in DBTT for JLF-1B is almost 70% larger than for JLF-1. The difference is attributed to the tenfold larger boron content prior to irradiation.

Keywords: neutron irradiation, ferritic-martensitic 7-9%Cr steels, low activation, tensile properties, fracture toughness, Charpy impact behavior, embrittlement, hardening, ductility

¹Materials scientists, NRG (former ECN), PO Box 25, 1755 ZG Petten, Netherlands.

²Professor, Dept. of Mech. and Environm. Engineering and Dept. of Chemical Engineering, University of California Santa Barbara, Santa Barbara, CA 93106.

³Professor, Dept. of Mech. and Environm. Engineering and Dept. of Materials, University of California Santa Barbara, Santa Barbara, CA 93106.

⁴The work reported is carried out and funded in the framework of the European Fusion Technology Program, and in the framework of the UCSB Program, funded by US-DOE.

Introduction

Reduced Activation Ferritic/Martensitic alloys are being developed for application in future thermonuclear fusion reactors by various partners in the fusion community. One of the major issues of these ferritic/martensitic alloys is the low temperature irradiation embrittlement. The irradiation behavior of the reduced activation martensitic steel F82H-mod (IEA heat), together with small amounts of other related alloys, such as JLF-1, JLF-1B or ORNL-9Cr2WVTa, was investigated by irradiation experiments in the High Flux Reactor (HFR) in Petten. Mechanical test specimens, such as tensile, KLST-type Charpy impact specimens and CT-specimens, were neutron irradiated to a dose level of 2–3 dpa at a temperature of 300°C.

Materials and Specimens

Materials

The materials studied are F82H, 7.5 and 15 mm plate from heat #9741 (also known as IEA Heat), and small amounts of JLF-1, JLF-1B, and ORNL-9Cr2WVTa. The chemical compositions are in Table 1. Details on the final heat treatment are given in Table 2. A common denominator of RAFM steels is the substitution of highly activating elements used in conventional ferritic/martensitic steels, e.g. molybdenum and niobium, with low or reduced activation elements such as tungsten, vanadium and tantalum.

JLF-1 and JLF-1B were produced in identical processes, and intended to obtain materials with virtually identical microstructure, essentially differing only in boron content. JLF-1B has a tenfold larger boron content than JLF-1. These alloys are used to study the effect of boron on hardening and embrittlement. Boron is a helium generating element, when irradiated with thermal neutrons. This is often used to generate fusion relevant helium concentrations in the steels, simulating the large amounts of helium generated by 14 MeV reactions in a thermonuclear fusion spectrum.

The structure of the steels is fully tempered martensitic. The temper treatment of all materials is aimed to obtain good toughness properties and keep sufficient tensile strength.

Specimens

Three types of specimens were used; cylindrical tensile specimens with a gage length of 20 mm and a diameter of 4 mm, miniaturized Charpy impact specimens KLST-type, and finally compact tension (CT) specimens of thickness of 10 mm. Drawings of each specimen type are presented in Fig. 1a to 1c. Tensile specimens were taken in the L orientation, CT and KLST specimens were taken in the L-T orientation, all with respect to the rolling direction.

Table 1 - *Chemical composition of materials*

Element	F82H-mod IEA heat 9741	JLF-1	JLF-1B	ORNL-9Cr2WVTa heat 3791
C	0.09	0.10	0.10	0.11
Si	0.11	0.05	0.04	0.21
Mn	0.16	0.45	0.46	0.44
P	0.002	<0.005	<0.005	0.015
S	0.002	0.0026	0.0027	0.008
Cr	7.71	8.88	8.87	8.9
Ni	0.02	-	-	<0.01
Mo	0.003	-	-	0.01
N	0.006	0.0215	0.0218	0.0215
Cu	0.01	-	-	0.03
Co	0.005	-	-	0.012
Ta	0.02	0.090	0.090	0.06
B	0.0002	0.0002	0.0022	<0.001
Ti	0.01	-	-	<0.01
Nb	0.0001	-	-	-
V	0.16	0.2	0.19	0.23
Al	0.003	-	-	0.017
W	1.95	1.95	1.94	2.01
Fe	bal.	bal.	bal.	bal.

Table 2 - *The final heat treatment, hardness and grain size of the FM steels*

	F82H-mod heat 9741	JLF-1	JLF-1B	ORNL- 9Cr2WVTa
Normalizing	1040°C/38min	1050°C/1h	1050°C/1h	1050°C/0.5h
Tempering	750°C/60min	780°C/1h	780°C/1h	750°C/1h
Hardness (HV5)	204	207	204	n.a.
Grain size (μm)	75	27±6	32±4	n.a.

n.a. not available

Irradiation Experiments

The specimens were irradiated in the HFR reactor in Petten. The irradiation capsules were of the type CHARIOT and ILAS, both targeted at a neutron dose level of 2.5 dpa at an irradiation temperature of 300°C. These capsules were instrumented with thermocouples for temperature monitoring and control, and with neutron monitor sets to determine accurately the accumulated dose and fluence profile over the capsule. The temperature of the capsule was controlled by adjusting the helium-neon cooling medium mixture. The axial temperature profile could be controlled by adjusting the

vertical position of the experiment in the HFR core. A summary of irradiation conditions is given in Table 3, details can be found in [1,2].

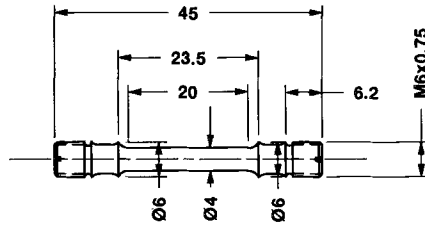


Figure 1a - Tensile test specimen

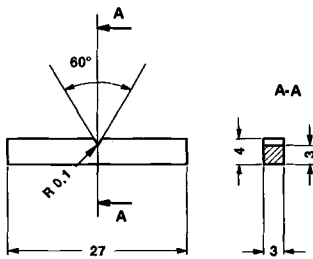


Figure 1b - Miniaturized Charpy impact specimen

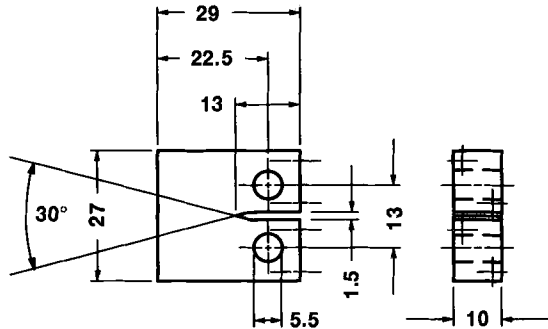


Figure 1c - CT-10 Compact tension specimen

The actual temperatures are indicated as ranges and are time-average values for the different locations within the experiment. The temperature averages are determined either from direct temperature measurements on the samples or by calculation on basis of measured specimen holder (drum) temperatures.

The displacement per atom dose was calculated from the neutron fluences, as derived from the activity measurement of the neutron fluence monitors contained in each experiment. The actual chemical composition of the sample materials as well as the irradiation history is taken in account to calculate the dpa-level.

Table 3 - Overview of irradiation experiments

Experiment	Specimen type	T_{irr} range (°C)	Dose (dpa)	Calculated helium content (appm)			
				F82H	JLF-1	JLF-1B	ORNL
ILAS-4	Tensile	325 – 335	2.4 - 3.0	2.7	2.8	23	<11
CHARIOT-2	CT-10mm, KLST	280 – 320	2.2 – 3.0	2.7	2.8	23	-

The formation of helium by transmutation reactions, in particular of boron, was also calculated with these neutron fluences (Table 3). As helium presumably plays an important role in the embrittlement behavior of the RAFM steels, and as boron is the largest contributor to the formation of helium for RAFM steels when irradiated in thermal and mixed spectrum reactors, the accuracy of the boron content is therefore of direct importance for the accuracy of helium content calculation. In past programs, investigating austenitic stainless steels, checks have been made with actual helium content measurements. The accuracy of the correspondence of the helium content and the content in boron and nickel was found to be satisfactory. For the current class of RAFM steels, who have very low boron contents, the accuracy of the boron content determination may be insufficient to determine the helium concentration by calculation alone, and should be checked by actual helium measurements.

The helium contents as stated in Table 3 are generated for 75% by the transmutation of ^{10}B in the case of F82H, JLF-1 and ORNL, and for 97% in the case of JLF-1B.

Mechanical Testing

Tensile Testing

The tensile experiments were performed on an electro-mechanical testing machine installed in the ECN Hot Cell Laboratory. The testing assembly was equipped with a 10 kN dynamic load cell and a two zone furnace. The tensile tests were performed with a constant actuator movement, resulting in a strain rate of $5 \times 10^{-4} \text{ s}^{-1}$. From the load-displacement curves strength data at specific plastic strain intervals were calculated. The 0.2% Yield Strength (0.2YS), the Ultimate Tensile Strength (UTS), Uniform Elongation (UE) and Total Elongation (TE) will be used here for presentation of results and discussion.

Charpy Impact Testing

Impact testing was performed on a instrumented and automated miniaturized impact tester, with a potential energy of 50 J and an impact speed of 3.85 m/s. Impact specimens can be tested automatically, at temperatures in the range of -150 to $+450^\circ\text{C}$. The results are presented in terms of impact energy. The impact energies are used to plot transition curves from which the ductile to brittle transition temperature (DBTT) and upper shelf energy (USE) for the material can be determined.

Fracture Toughness Testing

The post-irradiation fracture resistance experiments were performed on a servo-hydraulic testing machine, installed in a hot-cell. The test procedure is based on the ESIS P2-91 recommendation of the European Group on Fracture (EGF) for the single specimen J-resistance determination technique [3]. The load-line displacement is measured by

means of a strain-averaging system with two LVDTs. A separate direct current potential drop (DCPD) system is used for crack monitoring. The tests were performed in a two-zone furnace, in air environment after a temperature stabilization period of 30 minutes. Side-grooving after fatigue pre-cracking, as recommended in the ESIS procedure, is not performed with 10 mm CT specimens. The plane-sided specimens were fatigue pre-cracked at room temperature after irradiation. Automatic load shedding was applied for the K-controlled fatigue pre-cracking. Fatigue pre-cracking was done at 10 Hz with an R ratio of 0.1. The specimens that showed ductile tearing were heat-tinted after testing and then fractured by means of post test fatigue cracking at room temperature. The final DCPD crack length measurement is calibrated with the final crack length as measured on both fracture surfaces (weighted nine points averaging method).

In the brittle regime and in the transition regime, the K_Q is calculated according to ESIS-P2, which is practically identical to the ASTM E399 K_{Ic} procedure. Because of the test specimens size, the K_Q can not be promoted to K_{Ic} . In the ductile regime, the J-toughness is based on the ESIS-P2 approximation of J allowing for crack growth. The procedure differs from ASTM 1737 in the slope of the blunting line, which is used to determine the estimate of the initiation of stable crack propagation. This, in general, gives a somewhat lower value for the initiation toughness J_{02BL} than J_Q in the ASTM case. The material parameters used in this procedure are given in Table 4. The engineering estimate for onset of stable crack propagation J_{02bl} is subsequently converted to K-toughness by simple calculation.

Table 4 – Material properties used in the FTT evaluation, unirradiated and 2.5 dpa 300°C irradiated F82H-mod, 15 mm plate

	Unirradiated		2.5 dpa 300°C irradiated					
	24°C	325°C	24°C	50°C	80°C	100°C	150°C	325°C
0.2YS (MPa)	507	453	714	700	687	679	666	622
UTS (MPa)	629	520	762	742	724	714	694	640
E (GPa)	216	192	216	214	211	210	206	192
ν (-)	0.30	0.30	0.30	0.30	0.30	0.30	0.30	0.30

Results

Tensile Properties

Tensile tests were carried out in the range from room temperature to 550°C. The 0.2% yield stress, ultimate tensile strength and total and uniform elongation, for both unirradiated and irradiated specimens, are plotted as a function of test temperature in Figs 2-4. The results for F82H are in Fig 2, for both JLF-1 and JLF-1B in Fig 3, and finally the results for ORNL-9Cr2WVTa in Fig 4.

Irradiation hardening is observed for all four materials, and amounts to approximately 140 - 170 MPa at 300°C and 150 - 210 MPa at room temperature. F82H shows the most hardening, 170 MPa (Fig 2), and JLF-1 the least, 140 MPa (Fig 3). The

irradiation hardening is summarized in Table 5, for both room temperature and 300°C test temperatures. Further, the ductility was reduced by irradiation, approximately by 2.3-3.4 % for TE and 1.2-2.4 % for UE, tested at 300°C. The uniform elongation after irradiation remains above or just below 1% for all materials and all test temperatures. A limited amount of strain hardening capacity is still present after irradiation. F82H shows a minimum uniform elongation of 0.5 - 1% in the range of 200 to 500°C test temperatures. At test temperatures above 500°C, very little difference remains between the unirradiated and irradiated material; most of the irradiation hardening and loss of ductility was recovered at 550°C.

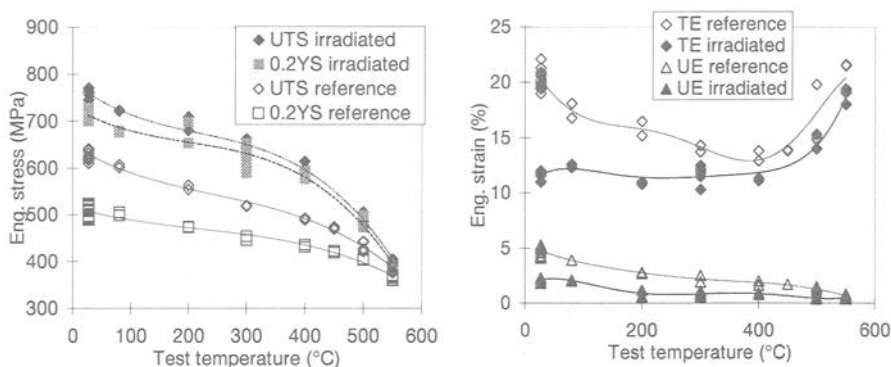


Figure 2 – Tensile properties of IEA F82H, heat 9741, before and after 2.5 dpa 300°C irradiation; (a) yield stress and ultimate strength, and (b) total and uniform elongation

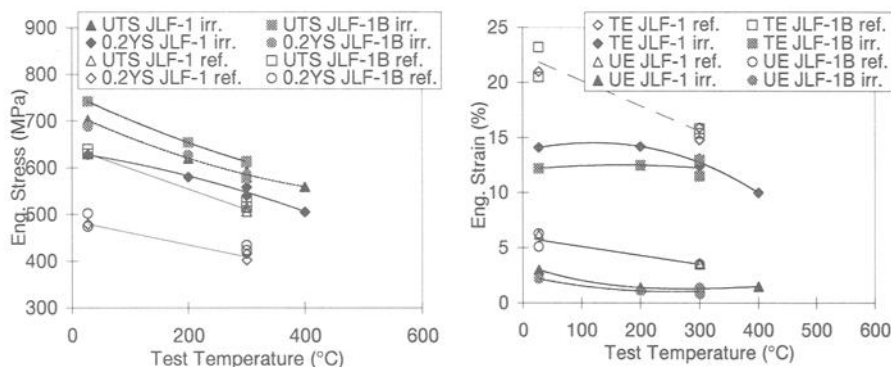


Figure 3 – Tensile properties of IEA JLF-1 and JLF-1B, before and after 2.5 dpa 300°C irradiation; (a) yield stress and ultimate strength, and (b) total and uniform elongation

In the unirradiated condition, JLF-1 and JLF-1B have almost identical tensile properties. After irradiation, and tested at room temperature, JLF-1B shows significantly more hardening than JLF-1; 200 versus 150 MPa. The loss of ductility is also more

pronounced for JLF-1B than for JLF-1. At 300°C test temperature, the differences are much smaller (Fig 3). The uniform elongation remains above 1% in the temperature range up to 400°C.

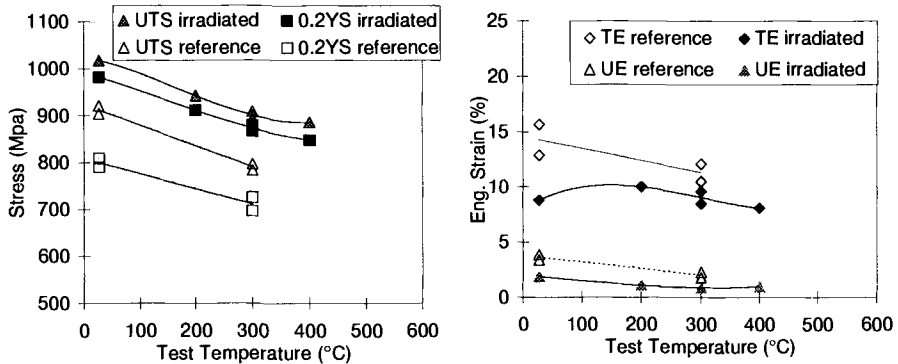


Figure 4 – Tensile properties of ORNL-9Cr2WVTa, before and after 2.5 dpa 300°C irradiation; (a) yield stress and ultimate strength and (b) total and uniform elongation

A remarkable point is the high strength of the ORNL steel, both in unirradiated and irradiated condition, (Fig 4). The ductility of this steel is lower than the other three steels. The uniform elongation after irradiation is minimally approximately 1%. The data for the unirradiated material correspond fairly well with properties measured by ORNL [4]. The reason for the higher tensile strength of this alloy is yet unresolved.

Table 5 - Overview of irradiation hardening and loss of ductility

	Tested at 27°C		Tested at 300°C	
	ΔYS (MPa)	ΔTE (%)	ΔYS (MPa)	ΔTE (%)
F82H	207	8.7	169	2.3
JLF-1	149	6.9	140	2.6
JLF-1B	200	9.6	153	2.3
ORNL	182	5.5	162	2.1

Miniaturized Charpy Impact Results

The Charpy impact test results are presented for both unirradiated and 2.5 dpa 300°C irradiated F82H-mod in Fig. 5. The results for JLF-1 and JLF-1B are in Fig. 6. The ORNL RAFM steel was not impact tested. The DBTT for unirradiated F82H lies around -95°C , whereas after irradiation, the DBTT has shifted to $+55^{\circ}\text{C}$, an irradiation induced shift of approximately 150°C . The DBTT of JLF-1 and JLF-1B in the unirradiated condition differ slightly; -112 and -100°C respectively. After irradiation the DBTT for JLF-1 lies at -25°C , a shift of approx. 90°C , whereas the DBTT for JLF-1B

after irradiation is around $+50^{\circ}\text{C}$, a shift of 150°C . The irradiation induced shift for JLF-1B is 60°C (66%) larger than for JLF-1.

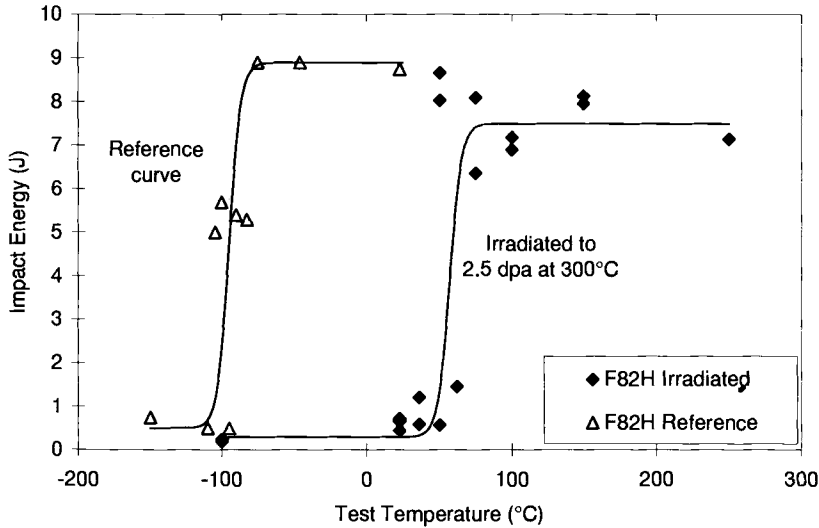


Figure 5 - Miniaturized Charpy (KLST) impact transition curves for unirradiated and 2.5 dpa 300°C irradiated F82H, IEA heat 9741

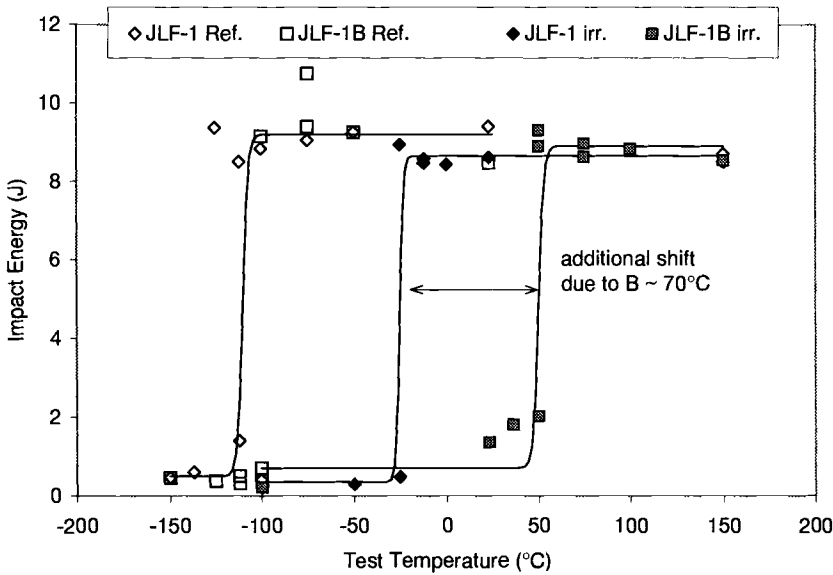


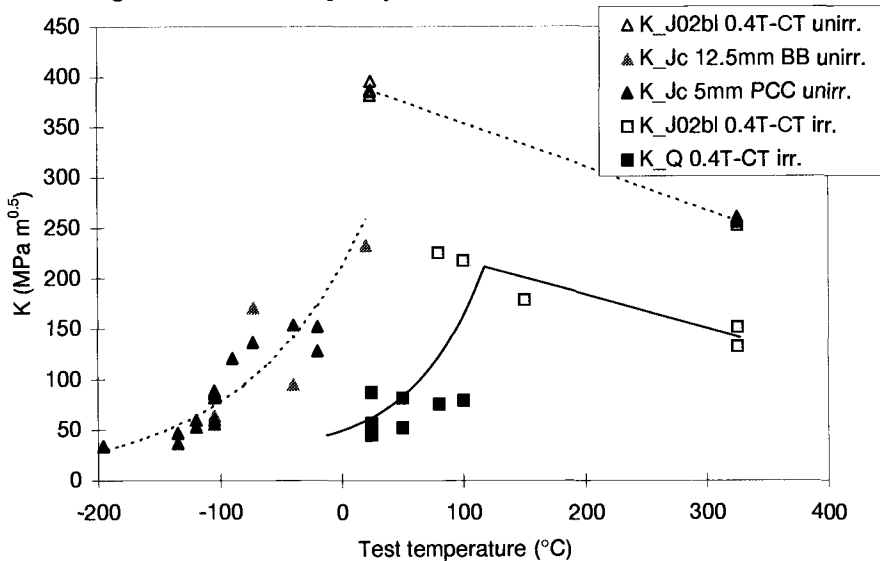
Figure 6 - Miniaturized Charpy (KLST) impact transition curves for unirradiated and 2.5 dpa 300°C irradiated JLF-1 and JLF-1B

The upper shelf energy (USE) of F82H is 8.9 J, after irradiation it is approximately 7.5 J, with a relatively large scatter. Hence, the reduction of USE is approximately 1.4 J for F82H. For both JLF-1 and JLF-1B, the USE is 9.2 J in the unirradiated condition. After irradiation, the USE is for both just a little lower, 0.6 and 0.3 J respectively.

It should be noted that for almost all upper shelf tests (unirradiated and irradiated, F82H and JLF-1, JLF-1B), the specimens were not broken by the impact.

Fracture Toughness Behavior

The results of the fracture toughness tests, carried out at ECN and at UCSB are plotted in Fig. 7 as a function of test temperature. Only F82H data were available. The datapoints are designated with K_{Jc} , K_Q , and K_{J02bl} , indicating by subscript the nature of the datapoint. K_{J02bl} is determined according to the ESIS procedure in the ductile regime, K_Q is determined according to the ESIS procedure for the brittle regime, and K_{Jc} is determined according to the ASTM procedure in the transition regime. The K_{Jc} data were supplied by UCSB, the K_Q and K_{J02bl} data by ECN. The UCSB data were produced with unirradiated 5 mm precracked charpies (PCC) and 12.5 mm bend bars (BB). The ECN data, were produced with 10 mm thick CT specimens, or 0.4T-CT. All 0.4T-CT tests showed either complete ductile tearing or cleavage fracture. No cases with noticeable crack extension before cleavage fracture were found. The tests with cleavage fracture were treated as brittle regime data in the K_Q calculation. The ductile regime data were treated to obtain J_{02bl} according to the ESIS standard. The J_{02bl} was subsequently converted to K_{J02bl} . The PCC and BB specimens were tested to obtain J_c data in the transition regime and were subsequently converted to K_{Jc} data.



The transition curve thus obtained with K_Q and K_{J02bl} , is qualitative transition curve, not a firm quantitative transition curve of one specific toughness parameter. The unirradiated F82H is fully ductile for the 0.4T-CT's from 325°C down to room temperature. The 5 mm PCC's and 12.5 mmBB's yield a DBTT (in terms of T_{K-100}) of approximately -70°C. After irradiation, the 0.4T-CT show brittle behavior up to 100°C, the DBTT is in the range of +80 to +100°C. The combination of these data indicates a shift in DBTT of approximately 160°C. The reduction of upper shelf energy by irradiation is found to be approximately 125 MPam^{0.5}.

Discussion

The four alloys are similar, but differ in a few aspects. Firstly, the chemical compositions are somewhat different (Table 1). F82H has low(est) chromium, manganese, nitrogen and tantalum contents, the ORNL RAFM steel has high(est) silicon, phosphorus and sulfur contents and intermediate tantalum, whereas the JLF-1 and JF-1B have low(est) silicon and high(est) tantalum. Finally, JLF-1B has highest boron content. The heat treatments are also similar but differences exist (Table 2). Hardness of F82H and JLF-1, 1B are similar, whereas the grain size of F82H is significantly larger than that of JLF-1, 1B (ORNL not available). F82H was produced on industrial scale, the other alloys were produced on laboratory scale. The specimens were irradiated at the same time in the same irradiation capsules.

Irradiation Hardening and Loss of Ductility

The tensile data (Fig 2,3,4 and Table 5), show that the irradiation hardening and loss of ductility behavior of the four alloys is approximately similar at 300°C. All show intermediate hardening in the range of 140-170 MPa, which is relatively low compared to results obtained with conventional 9Cr-steels [5]. More significant differences occur when tested at room temperature (Fig. 8). JLF-1B shows 50 MPa (33%) more irradiation hardening than JLF-1. A similar difference is present for the loss of ductility. The originally tenfold larger boron content of JLF-1B, transmuted by irradiation to helium (and lithium), seems to be the cause of an additional hardening and loss of ductility. At irradiation temperature however, this difference is not as pronounced.

Irradiation Hardening and DBTT shift for KLST specimens

The DBTT for F82H, JLF-1 and JLF-1B do not differ strongly in the unirradiated state (Fig 5,6 and Table 6). After irradiation however, the JLF-1 DBTT has shifted by 90°C, whereas JLF-1B DBTT has shifted by 150°C, approx. 66% more than JLF-1. This does suggest that the originally tenfold higher boron content, yielding tenfold higher helium content, does seriously affect the DBTT in irradiated state. F82H shows a shift similar to the high shift of JLF-1B, whereas the original boron content is low and similar to that of JLF-1, not to JLF-1B. Evidently, boron, or helium, is not the only factor affecting the embrittlement. One of the reasons for the difference between F82H and JLF-

l can be the larger grain size of F82H. The irradiation hardening of F82H and JLF-1B is similar at room temperature. The USE of JLF-1 is reduced slightly more than the USE of JLF-1B (Fig 6). It seems as if the higher hardening gives JLF-1B a slightly higher USE after irradiation. F82H does shows a much more pronounced degradation of the USE.

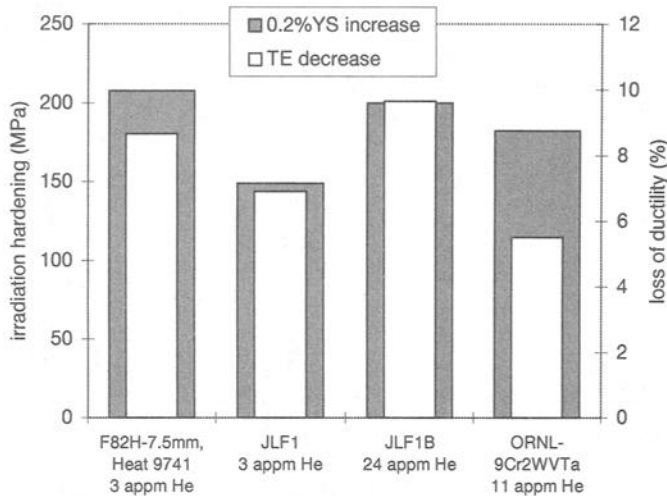


Figure 8 - Hardening and loss of ductility at 24°C after 2.5 dpa 300°C irradiation

Based on these comparisons, JLF-1 would be the best radiation resistant of the three RAFM alloys investigated here (ORNL excluded because of lack of data). The DBTT-shift is by far smallest for JLF-1, and its USE is only marginally affected. F82H might be called the worst of the three, given that the boron content was low, comparable to JLF-1, but showing an embrittlement behavior similar to the high boron content JLF-1B. A further disadvantage of F82H is the larger reduction of USE.

Table 6 - Overview of (shift in) DBTT and (reduction of) USE of F82H, JLF-1, and JLF-1B (KLST impact tests)

	Unirradiated		after 2.5 dpa 300°C		Change	
	DBTT (°C)	USE (J)	DBTT (°C)	USE (J)	ΔDBTT (°C)	ΔUSE (J)
F82H	-95	8.9	+55	7.5	+150	-1.4
JLF-1	-115	9.2	-25	8.6	+90	-0.6
JLF-1B	-100	9.2	+50	8.9	+150	-0.3

Static Fracture Toughness Tests

The qualitatively determined irradiation induced shift of DBTT of F82H in static fracture toughness tests corresponds fairly well to the value found for KLST impact tests,

both being approximately 150 to 160°C (Fig 5,7). The reduction of USE however, is much larger for the static fracture toughness tests than for impact tests; i.e. a 16% reduction for KLST impact and 45% for CT-10mm fracture toughness tests (Table 7). This suggests that considering the toughness degradation in terms of DBTT-shift or transition behavior alone is not sufficient. The USE apparently has a tendency to reduce to fairly low levels by irradiation (especially at higher test temperatures, Fig 7), possibly introducing toughness related complications even in the ductile regime. Evidently, one of the first priorities in developing RAFM steels is to avoid brittle behavior after irradiation, but consideration should be given to the ductile regime as well.

Table 7 – Comparison of USE at 100°C before and after irradiation for impact tests and static fracture toughness tests of F82H.

	USE unirr.	USE irradiated	Δ USE	Relative Δ USE
KLST impact test (J)	8.9	7.5	-1.4	-16%
CT fracture toughness (MPa $m^{0.5}$)	350	225	-125	-45%

Summary and Conclusions

Mechanical test specimens of four reduced activation alloys F82H-mod, JLF-1, JLF-1B and ORNL-9Cr2WVTa have been irradiated up to 2.5 dpa at 300°C. The observed irradiation hardening is largest for F82H and lowest for JLF-1. A small amount of strain hardening capacity remains for all four alloys after irradiation.

The radiation induced shift in DBTT for F82H is approximately 150 to 160°C, in miniaturized Charpy impact tests and static fracture toughness experiments. The upper shelf energy for static fracture toughness tests is almost halved after irradiation. The observed shift in DBTT and amount of irradiation hardening is fairly large, at least larger than expectations based on experience with the pre-IEA heat of F82H. However, the hardening and shift in DBTT is smaller than observed for many other (RA)FM alloys studied in fusion and fission programs.

JLF-1B, identical to JLF-1 but containing about ten times more boron before irradiation, behaves similarly to JLF-1 in the unirradiated condition. After irradiation however, the amount of helium generated in JLF-1B is significantly higher, causing a 60°C larger shift in DBTT for miniaturized Charpy impact tests, and 50 MPa higher irradiation hardening than JLF-1. Evidently, the tenfold larger helium content generated during irradiation is suspected to play an important role.

Comparing irradiation hardening and embrittlement of F82H, JLF-1 and JLF-1B, indicates JLF-1 as being the best radiation resistant of the three, and F82H slightly worse than JLF-1B because of larger USE reduction.

Acknowledgment

The authors wish to thank the following persons and institutions for the kind supply of materials: dr. A. Hishinuma, JAERI, for IEA heat F82H; drs A. Kohyama and Y. Kohno, University of Tokyo, for JLF-1 and JLF-1B; and dr. R.L Klueh, ORNL, for supply of ORNL-9Cr2WVTa.

References

- [1] D.J. Ketema, Neutron metrology in the HFR, Experiment ILAS-4, ECN-I-98-028, 1998.
- [2] J.H. Baard, Neutron Metrology in the HFR, Experiment CHARIOT-2, ECN-I-98-025, 1999.
- [4] R.L. Klueh, Metals and Ceramics Division, ORNL, personal communications April 1995 and May 1999.
- [3] ESIS Procedure for determining the Fracture Behaviour of Materials, ESIS P2-91.
- [5] M.G. Horsten et al., "Irradiation Behavior of Ferritic-Martensitic 9-12%Cr Steels," to be published in Effects of Radiation on Materials: 19th International Symposium, ASTM STP 1366.